

**Early changes in the extracellular matrix of the degenerating intervertebral disc, assessed by Fourier transform infrared imaging.**

EMANUEL, Kaj S, MADER, Kerstin T <<http://orcid.org/0000-0002-2524-6512>>, PEETERS, Mirte, KINGMA, Idsart, RUSTENBURG, Christine M E, VERGROESEN, Pieter-Paul A, SAMMON, Christopher <<http://orcid.org/0000-0003-1714-1726>> and SMIT, Theodoor H

Available from Sheffield Hallam University Research Archive (SHURA) at:

<http://shura.shu.ac.uk/21746/>

---

This document is the author deposited version. You are advised to consult the publisher's version if you wish to cite from it.

**Published version**

EMANUEL, Kaj S, MADER, Kerstin T, PEETERS, Mirte, KINGMA, Idsart, RUSTENBURG, Christine M E, VERGROESEN, Pieter-Paul A, SAMMON, Christopher and SMIT, Theodoor H (2018). Early changes in the extracellular matrix of the degenerating intervertebral disc, assessed by Fourier transform infrared imaging. *Osteoarthritis and cartilage*.

---

**Copyright and re-use policy**

See <http://shura.shu.ac.uk/information.html>

1 **Early changes in the extracellular matrix of the degenerating intervertebral disc,**  
2 **assessed by Fourier transform infrared imaging**

3  
4 Kaj S. Emanuel<sup>a,b</sup>, Kerstin T. Mader<sup>c</sup>, Mirte Peeters<sup>b</sup>, Idsart Kingma<sup>d</sup>, Christine M.E.  
5 Rustenburg<sup>a,b</sup>, Pieter-Paul A. Vergroesen<sup>b,e</sup>, Christopher Sammon<sup>c</sup>, Theodoor H. Smit<sup>a,f,\*</sup>

6 \*corresponding author

7 a - Department of Orthopaedic Surgery, Academic Medical Center, University of Amsterdam,  
8 Amsterdam Movement Sciences, Amsterdam, The Netherlands.

9 b – Department of Orthopedic Surgery, VU University Medical Center, Amsterdam  
10 Movement Sciences, The Netherlands

11 c – Materials and Engineering Research Institute, Sheffield Hallam University, Sheffield, UK

12 d – Department of Human Movement Sciences, Vrije Universiteit Amsterdam, Amsterdam  
13 Movement Sciences, The Netherlands

14 e – Department of Orthopaedic Surgery, NoordWest Ziekenhuisgroep, Alkmaar, The  
15 Netherlands

16 f – Department of Medical Biology, Academic Medical Center, University of Amsterdam,  
17 Amsterdam Movement Sciences, Amsterdam, The Netherlands.

18 \*Corresponding author at: Academisch Medisch Centrum, Postbus 22660, 1100DD  
19 Amsterdam, The Netherlands, tav. prof. dr. ir. T.H. Smit, Department of Medical Biology,  
20 [t.h.smit@amc.uva.nl](mailto:t.h.smit@amc.uva.nl)

21 Other authors:

22 Kaj Emanuel: [k.s.emanuel@amc.uva.nl](mailto:k.s.emanuel@amc.uva.nl)

23 Kirsten Mader: [k.mader@shu.ac.uk](mailto:k.mader@shu.ac.uk)

24 Mirte Peeters: [m.peeters@vumc.nl](mailto:m.peeters@vumc.nl)

25 Idsart Kingma: [i.kingma@vu.nl](mailto:i.kingma@vu.nl)

26 Christine Rustenburg: [c.rustenburg@vumc.nl](mailto:c.rustenburg@vumc.nl)

27 Pieter-Paul Vergroesen: [pvergroesen@gmail.com](mailto:pvergroesen@gmail.com)

28 Christopher Sammon: [c.sammon@shu.ac.uk](mailto:c.sammon@shu.ac.uk)

29

30 Running Title: Early matrix changes with disc degeneration

31

32 **Abstract**

33

34 Objective: Mechanical overloading induces a degenerative cell response in the intervertebral  
35 disc. However, early changes in the extracellular matrix (ECM) are challenging to assess with  
36 conventional techniques. Fourier Transform Infrared (FTIR) imaging allows visualization and  
37 quantification of the ECM. We aim to identify markers for disc degeneration and apply these  
38 to investigate early degenerative changes due to overloading and catabolic cell activity.

39 Design: Three experiments were conducted; Exp 1.: *In vivo*, lumbar spines of seven goats  
40 were operated: one disc was injected with chondroitinase ABC (mild degeneration) and  
41 compared to the adjacent disc (control) after 24 weeks. Exp 2a.: *Ex vivo*, caprine discs  
42 received physiological loading (n=10) or overloading (n=10) in a bioreactor. Exp 2b.: Cell  
43 activity was diminished prior to testing by freeze-thaw cycles, 18 discs were then tested as in  
44 Exp 2a. In all experiments, FTIR images (spectral region: 1000-1300  $\text{cm}^{-1}$ ) of mid-sagittal  
45 slices were analyzed using multivariate curve resolution.

46 Results: *In vivo*, FTIR was more sensitive than biochemical and histological analysis in  
47 identifying reduced proteoglycan content ( $p=0.046$ ) and increased collagen content in  
48 degenerated discs ( $p<0.01$ ). Notably, FTIR analysis additionally showed disorganization of  
49 the ECM, indicated by increased collagen entropy ( $p=0.011$ ).

50 *Ex vivo*, the proteoglycan/collagen ratio decreased due to overloading ( $p=0.047$ ) and collagen  
51 entropy increased ( $p=0.047$ ). Cell activity affected collagen content only ( $p=0.044$ ).

52 Conclusion: FTIR imaging allows a more detailed investigation of early disc degeneration  
53 than traditional measures. Changes due to mild overloading could be assessed and quantified.

54 Matrix remodeling is the first detectable step towards intervertebral disc degeneration.

55

56 Keywords: Fourier transform infrared; spectroscopy; intervertebral disc degeneration;  
57 overloading; collagen; entropy

58

59

60

## 61 **Introduction**

62

63 Intervertebral disc degeneration is a major cause of low-back pain<sup>1</sup>, which causes the most  
64 years lived with disability worldwide<sup>2</sup>. It is accepted that accumulating biomechanical  
65 overloading can initiate intervertebral disc degeneration<sup>3,4</sup>, but the pathophysiology is still  
66 under debate. On the one hand, it has been suggested that “repetitive loading can create  
67 microscopic damage within a material or tissue which gradually builds up until gross failure  
68 occurs”<sup>5</sup>. This assumes a passive role of the chondrocyte-like cells, which repair minor tissue  
69 damage, but would be unable to keep up with gross failure<sup>6</sup>. On the other hand, based on the  
70 many other factors that contribute to intervertebral disc degeneration (e.g. nutrient shortage,  
71 systemic inflammation, smoking), we hypothesized that disc degeneration is a vicious cycle<sup>7</sup>,  
72 where living cells interact with mechanical loading and extracellular matrix in a positive  
73 feedback loop (see Fig. 1). This is suggested by the observation that mild overloading of  
74 healthy intervertebral discs in a bioreactor results in katabolic (MMP13, ADAMTS5) and  
75 inflammatory gene expressions (IL-1, IL-8) by the resident chondrocytes<sup>8</sup>. Early changes in  
76 the extracellular matrix, however, are subtle and difficult to quantify by histology or magnetic  
77 resonance imaging (MRI).

78

79 Fourier transform infrared (FTIR) imaging was recently introduced as a method to visualize  
80 extracellular matrix composition of intervertebral discs on a tissue section without the need  
81 for staining<sup>9</sup>. With this method, the absorption of a range of frequencies of infrared light by  
82 thin slices of tissue is mapped. As different chemical bonds absorb light at different  
83 frequencies, information regarding the chemical composition can be obtained. This has  
84 several advantages over traditional histology, as this allows objective and quantitative  
85 measurement of the extracellular matrix composition. When the raw data can be deconvoluted  
86 into the dominant extracellular matrix types, such as proteoglycans and collagens, the  
87 distribution can be assessed in 2D on the same tissue sections, allowing ratio calculations.  
88 This has several advantages over the analysis of digitized histological staining. First, chemical  
89 contrast is generated without staining, which is therefore less affected by multiple sources of  
90 variations due to e.g. staining preparation and handling differences<sup>10</sup>. Furthermore, multiple  
91 ECM types can be quantified on the same slice, which enables ratio calculation. Altogether,  
92 FTIR imaging is a promising method to study more subtle changes in extracellular matrix  
93 than traditional measures, which would be necessary to study early changes with  
94 degeneration.

95

96 In this study, we first aimed to identify markers for degeneration based on FTIR imaging,  
97 using a validated *in vivo* goat model of mild degeneration<sup>11,12</sup>. The use of this model was  
98 necessary because healthy human control discs are rarely available for research. Secondly, we  
99 aimed to use these markers to detect early degenerative changes in *ex vivo* overloaded healthy  
100 goat intervertebral discs. We previously found upregulation of remodeling genes and  
101 downregulation of proteoglycan genes<sup>8</sup>. Here we hypothesize that proteoglycan content and  
102 structural integrity of the extracellular matrix are reduced in both the *in vivo* mildly  
103 degenerated discs and in the *ex vivo* overloaded discs. Our third aim was to assess the role of  
104 cell activity in early degeneration due to overloading. To that end, the *ex vivo* overloading  
105 experiment was repeated in an additional group while the cell activity was repressed in  
106 advance by freeze-thaw cycles. Since we hypothesize that changes in the extracellular matrix  
107 in response to overloading are cell-mediated (see Fig. 1), we expect less degenerative changes  
108 due to overloading in the group with suppressed cell activity.

109

## 110 **Methods**

111

### 112 *Experiment 1: in vivo degeneration with cABC*

113 Approval of the research protocol was obtained from the Animal Ethics Committee of the VU  
114 University Medical Center. Reporting of the experiment was conducted according to  
115 ARRIVE guidelines<sup>13</sup>. In each of seven healthy adult Dutch milk goats (age:  $3.8 \pm 1.5$  years) ,  
116 one lumbar intervertebral disc was injected with 0.25U chondroitinase ABC (cABC) per mL  
117 PBS in the nucleus pulposus using a 29G needle in the nucleus pulposus. This is a validated  
118 model for mild intervertebral disc degeneration<sup>11,12</sup>, as cABC cleaves proteoglycans in the  
119 nucleus pulposus. In every spine examined, one lumbar intervertebral disc served as a healthy  
120 control and was untreated. This resulted in seven healthy control discs and seven degenerated  
121 discs, which were used in this study. The goats were originally part of a treatment study, in  
122 which four additional lumbar discs received cABC injection and a hydrogel treatment twelve  
123 weeks later. After 12 more weeks, the goats were sacrificed. This study has been reported  
124 elsewhere<sup>14</sup>.

125

126 Midsagittal slices of the intervertebral discs were fixed in 4% formalin for 10 days,  
127 decalcified in Kristensens fluid for a week, embedded in paraffin, cut into 2  $\mu\text{m}$  sections and  
128 mounted onto stainless steel slides. Nucleus pulposus and annulus fibrosis material of the

129 remaining tissue was obtained for quantitative biochemistry. Glycosaminoglycan (GAG)  
130 content was measured using a 1,9-dimethyl-methylene blue (DMMB) assay (Biocolor Ltd)  
131 according to manufacturers' instructions. Hydroxyproline (HYP) content, a measure for total  
132 collagen content, was determined using a dimethylamino-benzaldehyde (DMBA)  
133 hydroxyproline assay. Histological analysis was done via Alcian Blue and H&E staining of  
134 midsagittal slices on a 6-point scale using the methods described elsewhere<sup>15</sup>.

135

### 136 *FTIR*

137 Mid-infrared spectroscopic images of the section on steel slides were measured with an  
138 Agilent 680-IR FTIR spectrometer, coupled to an Agilent 620-IR FTIR imaging microscope.  
139 The microscope was coupled with a liquid nitrogen cooled 64 × 64 mercury–cadmium–  
140 telluride focal plane array detector (FPA). Transflectance FTIR mosaic images (23 × 57  
141 images, pixel aggregation 256, image pixel dimensions: 92 × 228) were collected with a 4  
142 cm<sup>-1</sup> spectral resolution.

143

144 After manual exclusion of the bony parts, all scans were collated to one large data matrix.  
145 Data was pre-processed with custom-built code in MATLAB R2017a (IBM, The Mathworks,  
146 Inc., Natick, MA, USA). In summary, a second derivative was performed on the spectra  
147 (Savitzky–Golay: order 3, length 15). Furthermore, a tissue map was generated based on  
148 integration of the Amide III region (1297-1186 cm<sup>-1</sup>) in order to correct for tissue thickness  
149 variations. The data matrices were analyzed using a multivariate statistical methodology  
150 described by Mader *et al.*<sup>9</sup> They applied a MCR-ALS algorithm, which uses non-linear  
151 iterative partial least squares (NIPALS) decomposition and iterative alternating least-square  
152 optimization with soft non-negative constraints<sup>16</sup> (MCRv1.6 Copyright© 2003–2004 Unilever,  
153 UK). MCR-ALS analysis was carried out in a wavenumber range of 1000-1300 cm<sup>-1</sup> using the  
154 following settings: number of factors: 2; maximum number of iterations: 500; constraints:  
155 MALS-2D. The analyzed wavenumber region includes proteoglycan (SO<sup>3-</sup> antisymmetric  
156 stretching vibration, C-O stretching vibrations, C-O-S antisymmetric stretching vibrations)  
157 and collagen (amide III vibrations, C-O stretching vibrations) specific bonds,<sup>17</sup> which were  
158 used to determine the chemical identity of MCR-ALS factors. Additionally, calculated  
159 spectral MCR-ALS profiles were compared to the spectral profiles of reference materials  
160 collagen I, collagen II, chondroitin sulfate A, sodium salt and hyaluronic acid (all bovine)  
161 obtained from Sigma Aldrich (Gillingham, Dorset, UK). More details on the data analysis  
162 have been described elsewhere<sup>9</sup>. The calculated factors were averaged over the caudal-cranial

163 axis for 1D visualization and quantitative comparison. Further averaging over the anterior-  
164 posterior axis was used to obtain the average content of a matrix type. The structures were  
165 separated in nucleus pulposus and annulus fibrosis by manual selection of the region of  
166 interest (ROI) on the tissue map based on visual inspection. To quantify the disorganization of  
167 the collagen matrix, the distribution of the entire slice was analyzed by calculating the  
168 entropy, a standard texture analysis method of MATLAB. The entropy is defined as in  
169 Equation 1:

170

$$171 \quad Entropy = -\sum(p * \log_2(p)) \quad \text{Equation 1}$$

172

173 Where  $p$  contains the normalized histogram counts of the intensity of the MCR image factor.  
174 To analyze the local variations of the entropy, each intervertebral disc was divided in 10 equal  
175 parts from anterior to posterior, and the entropy was calculated for each part separately.

176

#### 177 *Experiment 2a: ex vivo degeneration using overloading*

178 Five spines of healthy Dutch Milk Goats were obtained from a local slaughterhouse. Within a  
179 few hours post-mortem, five lumbar intervertebral discs were removed from each spine  
180 (n=25) using an oscillating saw. Sawing debris was removed by flushing with PBS. One disc  
181 from each spine (n=5) did not receive any treatment and was immediately fixed in  
182 formaldehyde (t=0) after removal from the spine. The other four discs (n=20) were  
183 implemented in culture chambers of a custom-build Loaded Disc Culture System (LDCS).  
184 This LDCS allows application of axial compressive load to the intervertebral discs, as well as  
185 a constant flow of culture medium<sup>18</sup>. The intervertebral discs were cultured in standard culture  
186 medium (DMEM, Life Technologies) with added 10% Hyclone fetal bovine serum (FBS,  
187 Thermo Scientific ), 1% PSF, 3.5 g/L glucose (Merck), 25 mM HEPES buffer (Life  
188 Technologies) and 50 µg/ml ascorbate-2-phosphate (Sigma Aldrich).

189

190 From each spine, two randomly selected intervertebral discs were subjected to physiological  
191 loading (n=10), and two to overloading (n=10). Physiological loading was defined previously  
192 based on cage measures *in vivo* and was validated as a loading regime that maintained cell  
193 vitality, and induced no changes in gene expressions over the course of three weeks<sup>18</sup>. The  
194 physiological loading consisted of a dynamic daily regime of 8 hours of night time Low  
195 Dynamic Load (LDL) of  $50 \pm 10$  N, and then 16 hours of alternating 30 minutes of LDL and  
196 High Dynamic Load (HDL) of  $150 \pm 100$  N. The overloading loading regime is the same as

197 the physiological loading, except that the HDL phases are doubled in average force to  $300 \pm$   
198 100 N. The overloading was previously shown to induce katabolic and inflammatory gene  
199 expression<sup>8</sup>.

200

201 After three weeks of culturing with loading, the intervertebral discs were removed and  
202 midsagittal slices were mounted onto steel slides as in experiment 1. FTIR images were  
203 obtained as in experiment 1, other than that the microscope was coupled with a new larger  
204 128 x 128 FPA detector. Slices from the same intervertebral discs were processed for  
205 histological analysis using H&E, Safranin O and Masson's Trichrome staining. The sections  
206 were graded for degeneration by two independent observers, both using two different  
207 histological scales for intervertebral disc degeneration<sup>15,19</sup>.

208

#### 209 *Experiment 2b: reduced cell viability*

210 Experiment 2a was replicated with reduced cell viability, to test whether effects observed  
211 were due to cell activity. This is because extracellular matrix changes can occur in two ways:  
212 direct tissue damage due to the mechanical wear-and-tear, and biological adaptation due to  
213 mechanobiological cell activity. In order to address this, five additional lumbar goat spines  
214 were frozen at -20 °C for at least a month, including three freeze-thaw cycles. This group will  
215 be referred to as "non-vital", as cell viability is known to decrease drastically with this  
216 treatment<sup>20</sup>. The non-vital group was cultured in Phosphate Buffered Saline (PBS, Sigma  
217 Aldrich) only, with similar osmotic properties to culture medium, with 1% PSF added to  
218 prevent infection. All other steps and loading regimes were the same as applied to the vital  
219 group (Experiment 2a). If the changes with overloading, seen in Experiment 2a, do not occur  
220 in the group with reduced cell activity, the changes can be attributed to cell activity. If they do  
221 occur, it is due to mechanical wear-and-tear.

222

#### 223 *Statistics*

224 All statistical tests were performed in SPSS Statistics for Windows (Version 22; IBM Corp.,  
225 Armonk, NY). For each experiment, normality of the distribution of the FTIR parameters  
226 (average intensity or entropy) was investigated by visual inspection of QQ-plots and Shapiro-  
227 Wilk tests. The difference between parameters in experiment 1 was evaluated using a paired t-  
228 test, comparing the control and degenerated disc within each goat. The difference in  
229 histological score was evaluated using a signed rank test. The influence of loading regime on  
230 FTIR parameters in experiment 2a was analyzed using a linear mixed model. The model



231 included loading regime as fixed factor, because this is the independent variable we are  
232 interested in. It also included a random effect for each goat as a grouping factor, because  
233 multiple discs of each goat received the same loading regime, and therefore the discs within  
234 one subject are not independent. For experiment 2b, with the non-vital group added, vitality  
235 was added as fixed factor, as well as the interaction between loading group and vitality. This  
236 interaction models the influence of cell vitality on the effect of overloading. The difference  
237 between groups in the histological scores was evaluated using a Kruskal-Wallis test by ranks.

238

## 239 **Results**

240

### 241 *Experiment 1*

242 The increase in degeneration in the cABC injected discs compared to the control was  
243 confirmed on a 6-point histological grading score (median score [range]: 1 [0-4] vs 3 [1-5],  
244  $p=0.031$ ). Based on the GAG-assay of nucleus pulposus material, however, the difference  
245 between degenerated and control was not significant (365 vs 290 ug/mg  $p=0.11$ ). The  
246 differences between groups in the HYP content (25.6 vs 29.1 ug/mg,  $p=0.54$ ) and the  
247 GAG/HYP ratio (18.1 vs 11.1 g/g,  $p=0.21$ ) were not statistically significant. These data were  
248 reported elsewhere previously<sup>14</sup>.

249

250 In the FTIR MCR-ALS component analysis two factors for specific ECM types were  
251 identified. One factor showed the distribution of proteoglycans over the intervertebral disc.  
252 The average proteoglycan content in the nucleus showed a strong correlation ( $r=0.74$ ,  $p<0.01$ )  
253 with GAG content, measured with the bio-assay. The second factor that could be identified  
254 had a clear spectroscopic match with FTIR profiles of reference materials collagen-I and  
255 collagen-II (Fig. 2). The correlation between average collagen factor and hydroxyproline  
256 content was moderate ( $r=0.54$ ,  $p<0.05$ ). An overlay plot of the distribution of collagen and  
257 proteoglycan across the discs is shown in Fig. 3.

258

259 The average extracellular matrix content over the anterior-posterior axis is shown in Fig. 4.  
260 As expected, relatively more proteoglycan is found in the nucleus area, while more collagen is  
261 present in the outer annulus areas. All hereafter mentioned FTIR parameters (average  
262 intensity or entropy) were normally distributed. In the degenerated intervertebral discs,  
263 significantly less average proteoglycan was found compared to control discs, both overall  
264 ( $p=0.046$ ) and in the nucleus area ( $p=0.047$ ). The average collagen content was higher

265 (p<0.01) in the degenerated discs, both in the nucleus (p=0.027) and anterior annulus (p<0.01)  
266 (See Table 1). As a result, the proteoglycan/collagen ratio was also significantly reduced in  
267 degenerated discs compared to control, both overall (p=0.017) and in the anterior annulus  
268 (p=0.018). To test for disorganization of the collagen matrix, the distribution was analyzed by  
269 calculating the entropy. The collagen entropy was significantly higher in the degenerated  
270 discs (p=0.011). This means that a decrease of collagen organization is found in the  
271 degeneration group. The difference between the groups was most pronounced in the nucleus  
272 pulposus and anterior annulus areas (Table 3). A similar test of proteoglycan entropy  
273 differences did not reveal significant differences between the control and degenerated groups  
274 (p=0.70). Based on these results, the following FTIR markers for degeneration were selected  
275 for experiment 2: average proteoglycan content, increased collagen content, reduced  
276 proteoglycan/collagen ratio and increased collagen entropy.

277

#### 278 *Experiment 2a*

279 Due to damage to intervertebral discs during dissection and tissue damage during preparation  
280 for histology, analysis could not be completed for 2 intervertebral discs; therefore 23  
281 intervertebral discs remained.

282

283 No statistically significant differences between control loading, overloading, and t=0 (directly  
284 after sacrifice) were found in the scores based on conventional histological staining with  
285 Safranin O and H&E (Table 2, Fig. 5). All assessed FTIR parameters showed a normal  
286 distribution. The overloaded intervertebral discs had significantly higher collagen entropy  
287 than the control loaded intervertebral discs (p=0.047). No significant difference in overall  
288 average proteoglycan content (p=0.20), or collagen content (p=0.15) was found between the  
289 overloaded and control loaded discs (Fig. 6). However, the proteoglycan/collagen ratio was  
290 significantly lower in the overloaded group (p=0.047). Only whole-disc differences were  
291 significant. No significant difference between the control loaded group and the t=0 group was  
292 found in collagen or proteoglycan content or entropy (all p>0.05), although there was a trend  
293 towards higher collagen content in the control loaded group (p=0.075).

294

#### 295 *Experiment 2b*

296 To test whether cell activity modulates the effect of overloading, the experiment was  
297 replicated with the same loading conditions, but with reduced cell viability. In total, 18  
298 intervertebral discs were added to the analysis, in addition to the discs of experiment 2a. In

299 this extended dataset, significant main effects of overloading compared to control loading  
300 were found for collagen entropy ( $p=0.038$ ), average collagen content ( $p=0.036$ ) and average  
301 proteoglycan/collagen ratio ( $p=0.006$ ). The interaction between loading and vitality was only  
302 significant for the average collagen content ( $p=0.044$ ), with a trend towards an interaction for  
303 average proteoglycan/collagen ratio ( $p=0.059$ ), but not for proteoglycan content ( $p=0.67$ ) or  
304 collagen entropy ( $p=0.30$ ).

305

## 306 **Discussion**

307 Previously, it was shown that it was possible to detect several extracellular matrix types using  
308 FTIR imaging<sup>9</sup>. In the current study, the analysis of intervertebral discs was further developed  
309 to allow analysis of early disc degeneration, for which insufficiently sensitive markers exist to  
310 date. It was found that, from FTIR spectroscopic images of mid-sagittal slices, mild disc  
311 degeneration is related to reduced proteoglycan content, increased collagen content, and  
312 increased collagen entropy. Furthermore, after only three weeks of mild biomechanical  
313 overloading, a significant increase in entropy of the collagen factor and a decrease of average  
314 proteoglycan/collagen ratio could be detected. This indicates that the first steps into the  
315 vicious cycle of degeneration are related to the remodeling of the matrix, with a shift from  
316 proteoglycan-rich tissue to more fibrous collagen-rich tissue. At the same time, the  
317 organization in the collagen matrix is decreasing, as shown by an increase in entropy. The  
318 hypothesis that these changes are cell-mediated was not convincingly confirmed, as only the  
319 average collagen factor showed a significant interaction between the loading and vitality  
320 group; this implies that we found only minor support for a different response to loading due to  
321 reduced cell activity.

322

323 Control discs were compared to intervertebral discs treated with cABC injection to induce  
324 mild degeneration, a model that has been validated in several studies<sup>11,12,21</sup>. FTIR imaging  
325 showed a greater sensitivity to find differences between groups compared to traditional  
326 measures like histological grading and bio-assays. Possibly, the tissue samples for the bio-  
327 assay, taken from pieces of nucleus pulposus and annulus fibrosus just outside the midsagittal  
328 plane, were less representative compared to complete midsagittal slices. Furthermore, the  
329 GAG-assay only binds to the sulfated chains of proteoglycans, while the FTIR spectral  
330 signature includes the backbone and other non-sulfated proteoglycans, such as hyaluronic  
331 acid.

332

333 The proteoglycan-to-collagen ratio has been widely used as a marker for degenerative  
334 changes<sup>11,22,23</sup>. Using FTIR imaging, we found that with *in vivo* degeneration the proteoglycan  
335 factor/collagen factor ratio in the nucleus pulposus was reduced from 8.1 (control) to 3.7  
336 (mild degeneration). A statistically insignificant reduction was measured with the GAG/HYP  
337 assays: 18 vs 11. However, GAG/HYP ratio is an indirect measure for proteoglycan to  
338 collagen ratio, as GAG and HYP are only a small part of the proteoglycan and collagen  
339 molecules.

340

341 The most significant drawback of the current protocol is that the tissue is fixed in  
342 formaldehyde, which has a big absorption peak at  $1460\text{ cm}^{-1}$ , making it very difficult to  
343 include this region in the analysis, as the peak dominates the component analysis. However,  
344 the differences between the collagen type-I and type-II reference measurements are located  
345 exactly in this region<sup>9</sup>. A different conservation technique may improve the possibilities of  
346 matrix component identification. We speculate that the increase in collagen factor with  
347 degeneration, as found in this study, could be attributed to type-I collagen, as in previous  
348 work a strong upregulation of gene expression of collagen type-I in the nucleus pulposus was  
349 found with overloading, while the expression for collagen type-II was reduced<sup>8</sup>. The increase  
350 in entropy of the collagen factor may be a combination of newly formed collagen that is less  
351 attached to the highly-organized annulus fibrosis, and to the damaged collagen due to  
352 mechanical wear-and-tear or enzymatic cleavage. Future experiments with polarized light to  
353 determine the local orientation of the fibers, combined with immunohistochemical staining of  
354 multiple collagen types, may determine the contributions of the different processes. Recently,  
355 two studies were published that investigated the relation between degeneration and the  
356 heterogeneity of MRI signals in the intervertebral disc<sup>24,25</sup>, both indicating that the disorder of  
357 the extracellular matrix of the intervertebral disc is a relevant measure for disc degeneration.  
358 Furthermore, the intensity of the T2 signal on MRI, commonly used to determine disc  
359 degeneration, is dependent on the integrity and orientation of collagen fibers<sup>26,27</sup>. Therefore,  
360 the reduction in T2 signal, as found with mild degeneration<sup>28</sup> could be partly attributed to the  
361 increasing entropy of the collagen network.

362

363 The effect of overloading on the matrix of the intervertebral disc was subtle in this study, as  
364 traditional histology could not distinguish between overloaded and control-loaded groups.  
365 This was unexpected, as previous work did show a significant difference in gene expressions  
366 that indicated remodeling of the matrix<sup>8</sup>. Matrix breakdown is however a slow process,

367 because the cell density in the intervertebral disc is very low<sup>29</sup>. The turnover rate for  
368 proteoglycans in the intervertebral disc is estimated at roughly 5% per year<sup>30</sup>; for collagen,  
369 rates between 0.3 and 0.7 % are reported<sup>31</sup>. Therefore, an overloading period longer than three  
370 weeks or a more intense overloading regime may be needed for future studies to provide a  
371 more robust outcome.

372

373 The hypothesis that initiation of intervertebral disc degeneration is cell-mediated was not  
374 confirmed. If the effect of overloading is different in the vital groups compared to the non-  
375 vital groups, this would be expressed in the statistical model as an interaction between loading  
376 group and vitality. In the measures which were significantly different between the overloading  
377 and control loading in the vital intervertebral discs, no significant interaction was found. The  
378 average collagen factor content did show a significant interaction, which is not surprising  
379 when considering that cell activity is needed to increase the collagen content. It is unclear,  
380 however, if the increase in collagen entropy and break-down of proteoglycans, as observed in  
381 the vital group, are also mediated by cell activity. The absence of the interaction between  
382 loading group and vitality in these measures did not indicate that. The vitality was reduced by  
383 three freeze-thaw cycles, and the cell activity was further reduced by culturing on PBS instead  
384 of culture medium. Three freeze-thaw cycles at -20 °C was shown to kill 100% of  
385 chondrocytes in articular cartilage<sup>20</sup>.

386

387 The transferability of the spectral factors between the *in vivo* experiment and the bioreactor  
388 studies, despite a slightly different scanning setup, is an important finding, as this is a  
389 requirement for wider implementation. A limitation in the current study is the use of goat  
390 intervertebral discs. The use of an animal model is necessary in the study of healthy  
391 intervertebral discs, as healthy human tissue is not readily available. The bioreactor studies  
392 reduce the use of animal models, as only waste products of the slaughterhouse are needed.  
393 The goat is used as a model because goat intervertebral discs do not contain notochordal cells,  
394 similar to the adult human intervertebral disc<sup>32</sup>. Furthermore, quadrupeds are a useful model  
395 biomechanically, despite their horizontal alignment<sup>33</sup>. For the application of the load on the  
396 intervertebral discs in the bioreactor, it was decided to not correct for size of the disc, as the  
397 mid-sagittal area was unknown at before the start of the experiments and the bone area may  
398 not be a reliable estimate of size differences. In previous research with the same goat  
399 population, the mid-sagittal area differences were relatively small: 4.35+/-0.46 cm<sup>2</sup>.<sup>34</sup>  
400 Furthermore, no bias was introduced as intervertebral discs were randomly allocated to the

401 different groups. Another limitation is that the FTIR measures in this study have no unit, and  
402 are therefore not directly comparable to other studies. Future studies on the relation between  
403 these measures and proteoglycan and collagen concentration should enable the conversion to  
404 actual concentration. Another important limitation is that this method is not applicable in the  
405 clinical setup, as intervertebral disc tissue cannot be obtained without damaging the  
406 intervertebral disc. There is a great need for the improvement of current clinical imaging of  
407 intervertebral disc degeneration. The currently most-used clinical imaging method, the MRI-  
408 based Pfirrmann Score<sup>35</sup>, is widely regarded as unsatisfactory due to low discriminative power  
409 and subjective nature<sup>36,37</sup>. However, to improve this gold standard, new MRI techniques need  
410 to be validated against relevant, quantitative measures for intervertebral disc degeneration,  
411 which are currently unavailable. Developing measures that can be used in research will  
412 eventually facilitate the improvement of clinical measures. With FTIR spectroscopic imaging  
413 it is possible to describe the process of degeneration in a more detailed and quantitative  
414 manner, and therefore it could serve as a potential benchmark for clinical imaging methods.

415

416 In conclusion, FTIR imaging provides quantitative, sensitive measures to study early changes  
417 in extracellular matrix with intervertebral disc degeneration. This is an important step  
418 forward, as such measures are necessary to be able to study the etiology of intervertebral disc  
419 or cartilage degeneration. Reduction in proteoglycan factor, increase in collagen factor,  
420 decrease of the proteoglycan/collagen ratio and increase in the collagen entropy were shown  
421 to be measures for intervertebral disc degeneration. After three weeks of overloading, the  
422 proteoglycan/collagen factor ratio was reduced, and the collagen entropy increased. Our study  
423 is inconclusive about whether this process is cell-mediated.

424

#### 425 **Role of funding sources.**

426

427 The authors acknowledge the financial support of the Task Force of Research of  
428 EUROSPINE and COST-Action MP1302: Nanospectroscopy. The sponsors were not  
429 involved in the experiment or manuscript submission.

430

#### 431 **Competing interests**

432

433 None of the authors reported conflicts of interest.

434

435 **Author contributions**

436

437 KE, PV, IK, MP & TS designed the experiments. KE, MP & CR conducted the experiments.  
438 KE, KM & CS performed FTIR analysis. KE, IK, KM, CS & TS analyzed overall results. KE  
439 drafted the manuscript. All authors critically reviewed the manuscript and approved the final  
440 version.

441

442 **References**

443

- 444 1. Brinjikji W, Diehn F, Jarvik J, Carr C, Kallmes DF, Murad MH, et al. MRI findings of  
445 disc degeneration are more prevalent in adults with low back pain than in  
446 asymptomatic controls: a systematic review and meta-analysis. *American Journal of*  
447 *Neuroradiology*. 2015;36(12):2394-2399. 10.3174/ajnr.A4498
- 448 2. Vos T, Flaxman AD, Naghavi M, Lozano R, Michaud C, Ezzati M, et al. Years lived  
449 with disability (YLDs) for 1160 sequelae of 289 diseases and injuries 1990–2010: a  
450 systematic analysis for the Global Burden of Disease Study 2010. *The Lancet*.  
451 2013;380(9859):2163-2196.
- 452 3. Chan SC, Ferguson SJ, Gantenbein-Ritter B. The effects of dynamic loading on the  
453 intervertebral disc. *Eur Spine J*. 2011;20(11):1796-1812. 10.1007/s00586-011-1827-1
- 454 4. Hung YJ, Shih TT, Chen BB, Hwang YH, Ma LP, Huang WC, et al. The dose-  
455 response relationship between cumulative lifting load and lumbar disk degeneration  
456 based on magnetic resonance imaging findings. *Phys Ther*. 2014;94(11):1582-1593.  
457 10.2522/ptj.20130095
- 458 5. Adams MA. Biomechanics of back pain. *Acupuncture in Medicine*. 2004;22(4):178-  
459 188. 10.1136/aim.22.4.178
- 460 6. Coenen P, Kingma I, Boot CR, Bongers PM, van Dieën JH. The contribution of load  
461 magnitude and number of load cycles to cumulative low-back load estimations: a  
462 study based on in-vitro compression data. *Clinical Biomechanics*. 2012;27(10):1083-  
463 1086. 10.1016/j.clinbiomech.2012.07.010
- 464 7. Vergroesen PP, Kingma I, Emanuel KS, Hoogendoorn RJ, Welting TJ, van Royen BJ,  
465 et al. Mechanics and biology in intervertebral disc degeneration: a vicious circle.  
466 *Osteoarthritis Cartilage*. 2015;23(7):1057-1070. 10.1016/j.joca.2015.03.028
- 467 8. Paul CP, Schoorl T, Zuiderbaan HA, Zandieh Doulabi B, van der Veen AJ, van de  
468 Ven PM, et al. Dynamic and static overloading induce early degenerative processes in  
469 caprine lumbar intervertebral discs. *PLoS One*. 2013;8(4):e62411.  
470 10.1371/journal.pone.0062411
- 471 9. Mader KT, Peeters M, Detiger SE, Helder MN, Smit TH, Le Maitre CL, et al.  
472 Investigation of intervertebral disc degeneration using multivariate FTIR  
473 spectroscopic imaging. *Faraday discussions*. 2016;187:393-414. 10.1039/c5fd00160a
- 474 10. Hyllested J, Veje K, Ostergaard K. Histochemical studies of the extracellular matrix of  
475 human articular cartilage—a review. *Osteoarthritis and cartilage*. 2002;10(5):333-  
476 343.
- 477 11. Hoogendoorn RJ, Helder MN, Kroeze RJ, Bank RA, Smit TH, Wuisman PI.  
478 Reproducible long-term disc degeneration in a large animal model. *Spine*.  
479 2008;33(9):949-954. 10.1097/BRS.0b013e31816c90f0
- 480 12. Gullbrand S, Malhotra N, Schaer T, Zawacki Z, Martin J, Bendigo J, et al. A large

- 481 animal model that recapitulates the spectrum of human intervertebral disc  
482 degeneration. *Osteoarthritis and Cartilage*. 2017;25(1):146-156.  
483 10.1016/j.joca.2016.08.006
- 484 13. Kilkenny C, Browne WJ, Cuthill IC, Emerson M, Altman DG. Improving bioscience  
485 research reporting: the ARRIVE guidelines for reporting animal research. *PLoS*  
486 *biology*. 2010;8(6):e1000412.
- 487 14. Peeters M, Detiger SE, Karfeld-Sulzer LS, Smit TH, Yayon A, Weber FE, et al. BMP-  
488 2 and BMP-2/7 heterodimers conjugated to a fibrin/hyaluronic acid hydrogel in a large  
489 animal model of mild intervertebral disc degeneration. *BioResearch open access*.  
490 2015;4(1):398-406. 10.1089/biores.2015.0025
- 491 15. Hoogendoorn RJ, Wuisman PI, Smit TH, Everts VE, Helder MN. Experimental  
492 intervertebral disc degeneration induced by chondroitinase ABC in the goat. *Spine*.  
493 2007;32(17):1816-1825. 10.1097/BRS.0b013e31811ebac5
- 494 16. Wang J-H, Hopke PK, Hancewicz TM, Zhang SL. Application of modified alternating  
495 least squares regression to spectroscopic image analysis. *Analytica Chimica Acta*.  
496 2003;476(1):93-109.
- 497 17. Rieppo L, Saarakkala S, Narhi T, Helminen HJ, Jurvelin JS, Rieppo J. Application of  
498 second derivative spectroscopy for increasing molecular specificity of Fourier  
499 transform infrared spectroscopic imaging of articular cartilage. *Osteoarthritis*  
500 *Cartilage*. 2012;20(5):451-459. 10.1016/j.joca.2012.01.010
- 501 18. Paul CP, Zuiderbaan HA, Zandieh Doulabi B, van der Veen AJ, van de Ven PM, Smit  
502 TH, et al. Simulated-physiological loading conditions preserve biological and  
503 mechanical properties of caprine lumbar intervertebral discs in ex vivo culture. *PLoS*  
504 *One*. 2012;7(3):e33147. 10.1371/journal.pone.0033147
- 505 19. Sive J, Baird P, Jeziorski M, Watkins A, Hoyland J, Freemont A. Expression of  
506 chondrocyte markers by cells of normal and degenerate intervertebral discs. *Molecular*  
507 *Pathology*. 2002;55(2):91.
- 508 20. Clements K, Bee Z, Crossingham G, Adams M, Sharif M. How severe must repetitive  
509 loading be to kill chondrocytes in articular cartilage? *Osteoarthritis and Cartilage*.  
510 2001;9(5):499-507. 10.1053/joca.2000.0417
- 511 21. Detiger SE, Hoogendoorn RJ, van der Veen AJ, van Royen BJ, Helder MN,  
512 Koenderink GH, et al. Biomechanical and rheological characterization of mild  
513 intervertebral disc degeneration in a large animal model. *J Orthop Res*.  
514 2013;31(5):703-709. 10.1002/jor.22296
- 515 22. Emanuel KS, Vergroesen P-PA, Peeters M, Holewijn RM, Kingma I, Smit TH.  
516 Poroelastic behaviour of the degenerating human intervertebral disc: a ten-day study in  
517 a loaded disc culture system. *European Cells and Materials*. 2015;29:330-341.  
518 10.22203/eCM.v029a25
- 519 23. Mwale F, Roughley P, Antoniou J. Distinction between the extracellular matrix of the  
520 nucleus pulposus and hyaline cartilage: a requisite for tissue engineering of  
521 intervertebral disc. *Eur Cell Mater*. 2004;8(58):63-64. 10.22203/eCM.v008a06
- 522 24. Waldenberg C, Hebelka H, Brisby H, Lagerstrand KM. MRI histogram analysis  
523 enables objective and continuous classification of intervertebral disc degeneration.  
524 *European Spine Journal*. 2017:Pub. ahead of Print. 10.1007/s00586-017-5264-7
- 525 25. Pandit P, Talbott JF, Padoa V, Dillon W, Majumdar S. T1ρ and T2-based  
526 characterization of regional variations in intervertebral discs to detect early  
527 degenerative changes. *Journal of Orthopaedic Research*. 2016;34(8):1373-1381.
- 528 26. Xia Y, Farquhar T, Burton-Wurster N, Lust G. Origin of cartilage laminae in MRI.  
529 *Journal of Magnetic Resonance Imaging*. 1997;7(5):887-894.
- 530 27. Shao H, Pauli C, Li S, Ma Y, Tadros AS, Kavanaugh A, et al. Magic angle effect



- 531 plays a major role in both T1rho and T2 relaxation in articular cartilage. *Osteoarthritis*  
532 *and Cartilage*. 2017;25(12):2022-2030. 10.1016/j.joca.2017.01.013
- 533 28. Luoma K, Vehmas T, Riihimaki H, Raininko R. Disc height and signal intensity of the  
534 nucleus pulposus on magnetic resonance imaging as indicators of lumbar disc  
535 degeneration. *Spine*. 2001;26(6):680-686. Doi 10.1097/00007632-200103150-00026
- 536 29. Liebscher T, Haefeli M, Wuertz K, Nerlich AG, Boos N. Age-related variation in cell  
537 density of human lumbar intervertebral disc. *Spine*. 2011;36(2):153-159.
- 538 30. Sivan SS, Tsitron E, Wachtel E, Roughley PJ, Sakkee N, van der Ham F, et al.  
539 Aggrecan turnover in human intervertebral disc as determined by the racemization of  
540 aspartic acid. *Journal of Biological Chemistry*. 2006;281(19):13009-13014.
- 541 31. Sivan S-S, Wachtel E, Tsitron E, Sakkee N, van der Ham F, DeGroot J, et al. Collagen  
542 turnover in normal and degenerate human intervertebral discs as determined by the  
543 racemization of aspartic acid. *Journal of Biological Chemistry*. 2008;283(14):8796-  
544 8801.
- 545 32. Vonk LA, Kroeze RJ, Doulabi BZ, Hoogendoorn RJ, Huang C, Helder MN, et al.  
546 Caprine articular, meniscus and intervertebral disc cartilage: an integral analysis of  
547 collagen network and chondrocytes. *Matrix Biol*. 2010;29(3):209-218.  
548 10.1016/j.matbio.2009.12.001
- 549 33. Smit TH. The use of a quadruped as an in vivo model for the study of the spine -  
550 biomechanical considerations. *Eur Spine J*. 2002;11(2):137-144.  
551 10.1007/s005860100346
- 552 34. Emanuel KS, van der Veen AJ, Rustenburg CM, Smit TH, Kingma I. Osmosis and  
553 viscoelasticity both contribute to time-dependent behaviour of the intervertebral disc  
554 under compressive load: A caprine in vitro study. *Journal of Biomechanics*.  
555 2017;70:10-15.
- 556 35. Pfirrmann CW, Metzdorf A, Zanetti M, Hodler J, Boos N. Magnetic resonance  
557 classification of lumbar intervertebral disc degeneration. *Spine*. 2001;26(17):1873-  
558 1878.
- 559 36. Adams MA, Roughley PJ. What is intervertebral disc degeneration, and what causes  
560 it? *Spine*. 2006;31(18):2151-2161.
- 561 37. Videman T, Battié MC, Gibbons LE, Gill K. A new quantitative measure of disc  
562 degeneration. *The Spine Journal*. 2017;17(5):746-753. 10.1016/j.spinee.2017.02.002  
563  
564

565 **Figure 1.** The vicious cycle of intervertebral disc degeneration. Biomechanical signals can  
566 induce cellular remodeling of the extracellular matrix, which in turn changes the  
567 biomechanical properties. Reprinted from Vergroesen et al.,<sup>7</sup> with permission from Elsevier.

568 **Figure 2.** Left: Spectral profiles of proteoglycan factor, received from the MCR analysis of  
569 experiment 1, compared to spectral profiles of reference hyaluronic acid and chondroitin  
570 sulfate. Right: spectral profile of collagen with reference measurements of pure collagen I and  
571 II.

572  
573 **Figure 3.** Example of overlay plots of proteoglycan factor (green) and collagen factor (red),  
574 scaled on RGB from 0 to 255 (255 is the highest value seen in all intervertebral discs).

575 **Figure 4.** Average distribution of the proteoglycan factor (top) and collagen factor (bottom)  
576 over percentage of width from anterior to posterior with SEM in color.

577  
578 **Figure 5.** Left: distribution of the proteoglycan factor for four intervertebral discs of  
579 experiment 2. Right: Safranin O staining of nearby slices of the same four intervertebral discs.  
580 With this staining, proteoglycans are shown in red.

581  
582 **Figure 6.** Average proteoglycan and collagen factor over percentage of width from anterior to  
583 posterior, with SEM in color.

584

585 **Table 1.** Average proteoglycan and collagen content Experiment 1

	Whole disc control	Whole disc degenerated	Difference [95% CI]	Nucleus control	Nucleus degenerated	Difference nucleus [95% CI]	Anterior annulus control	Anterior annulus degenerated	Difference anterior annulus [95% CI]
Average Proteoglycan content	0.224	0.179	-0.045 [-0.09,- 0.00]	0.302	0.242	-0.060 [-0.119,- 0.001]	0.080	0.061	-0.019 [-0.038, 0.000]
Average Collagen content	0.054	0.086	0.031 [0.013,0.05]	0.0437	0.0751	0.0314 [-0.058,- 0.005]	0.071	0.111	-0.040 [-0.0150, - 0.0642]
Proteoglycan/ Collagen ratio	4.38	2.26	-2.12 [-3.73, -0.52]	8.17	3.71	-4.46 [-9.11,- 0.19]	1.41	0.58	-0.84 [-1.47,- 0.20]

586

587 **Table 2.** Median [minimum-maximum] for the histological degenerative gradings.  
588 Safranin O histological staining on nearby slices of the same intervertebral disc (Fig. 5)  
589 showed similar distribution as the intervertebral discs from experiment 2, confirming that this  
590 factor indeed identifies proteoglycan.

Loading group	Method by Hoogendoorn et al. <sup>11</sup>	Method by Sive et al. <sup>19</sup>
Control loading	2.3 [0.0-3.0]	2.0 [1.0-3.5]
Overloading	2.3 [0.5-3.5]	1.3 [0.5-3.0]
T=0	1.8 [0.0-2.5]	1.8 [1.0-3.0]

591

592

593 **Table 3.** Collagen entropy of different sections of the discs of experiment 1, divided into 10  
 594 equal parts from anterior to posterior.

Percentile anterior-posterior width	Entropy healthy (SD)	Entropy degenerated (SD)	P-value
0-10	4.3 (0.8)	5.1 (0.3)	0.06
10-20	4.4 (0.7)	5.3 (0.3)	0.03
20-30	3.3 (0.6)	4.6 (0.4)	<0.01
30-40	3.0 (0.8)	4.0 (0.5)	0.01
40-50	3.0 (0.8)	4.1 (0.5)	0.04
50-60	2.9 (1.1)	4.1 (0.7)	0.07
60-70	3.2 (1.3)	4.0 (0.4)	0.13
70-80	3.4 (0.7)	3.8 (0.5)	0.05
80-90	3.7 (0.8)	3.7 (0.3)	0.81
90-100	1.7 (1.9)	1.6 (2.0)	0.92

595  
 596

Figure 1  
Click here to download high resolution image

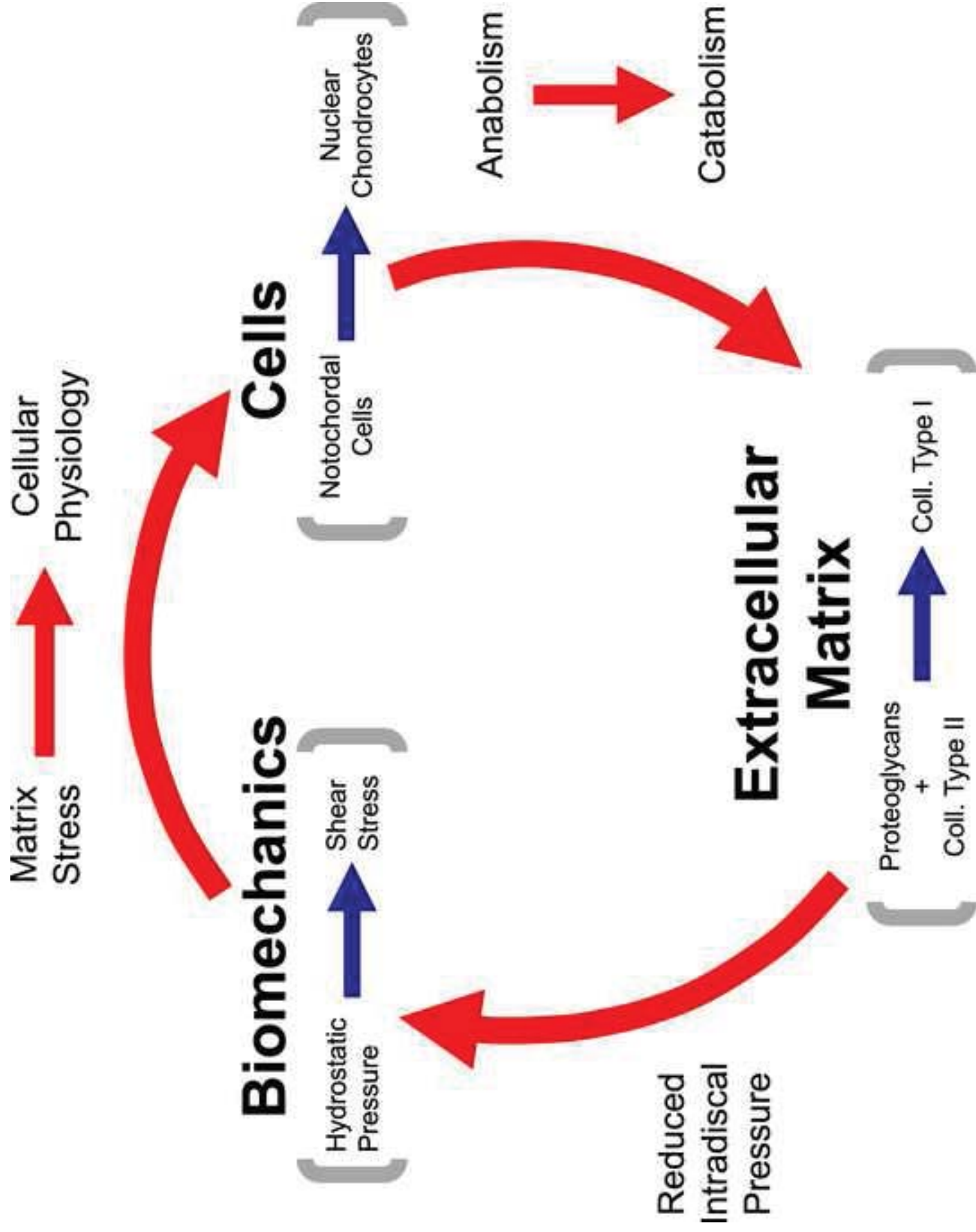


Figure 2a  
[Click here to download high resolution image](#)

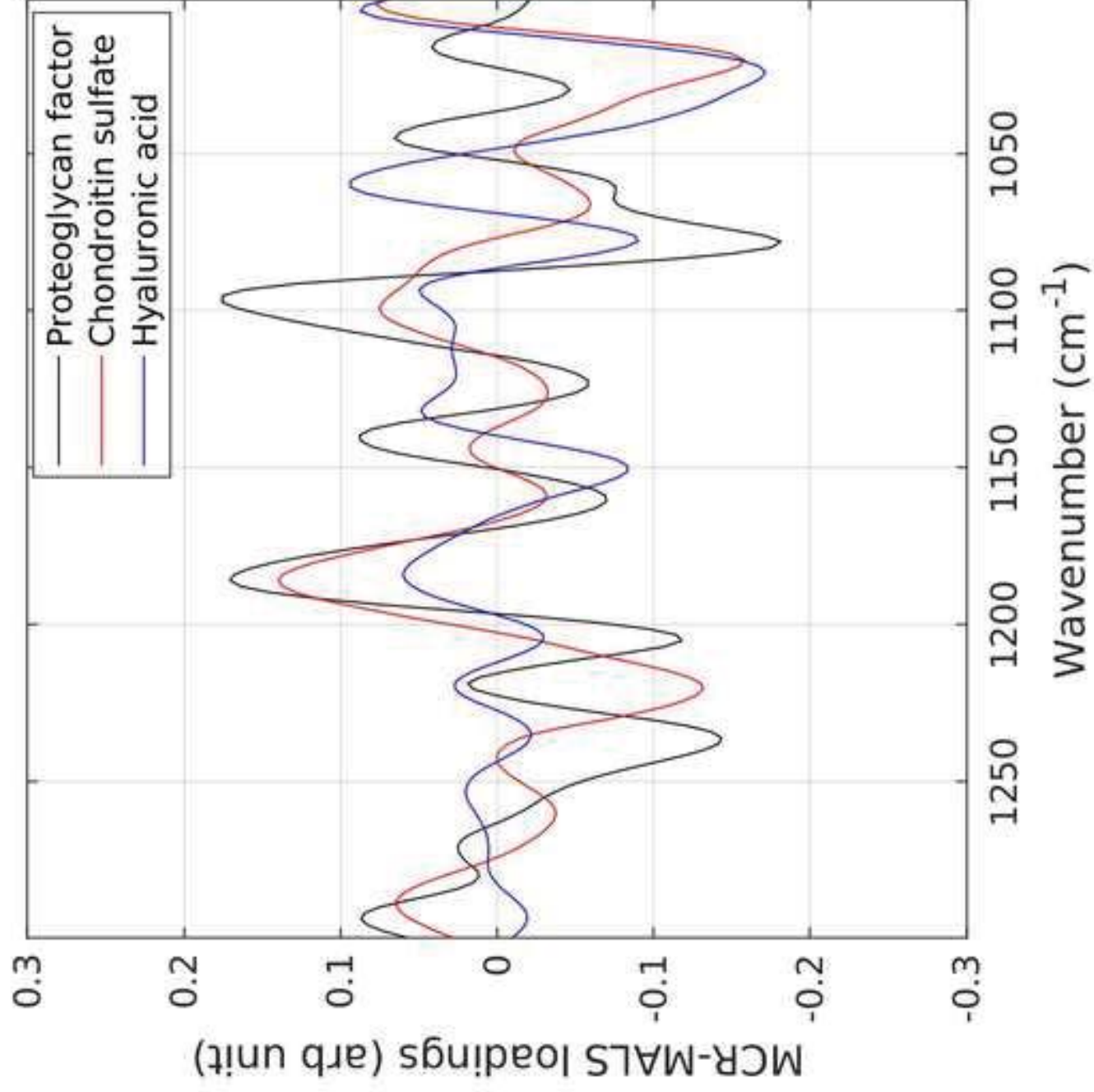


Figure 2b  
[Click here to download high resolution image](#)

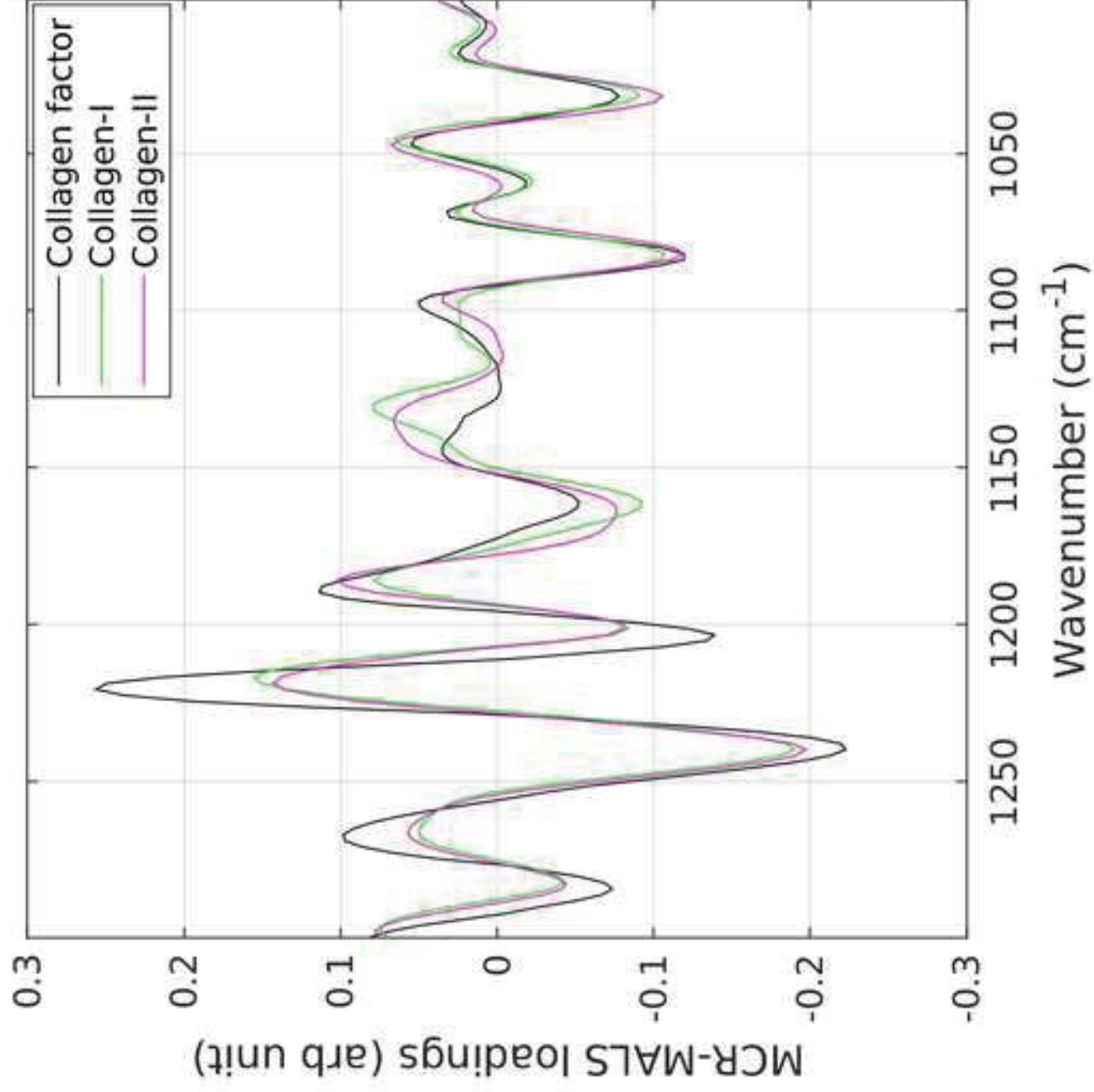




Figure 3  
[Click here to download high resolution image](#)



Figure 4  
[Click here to download high resolution image](#)

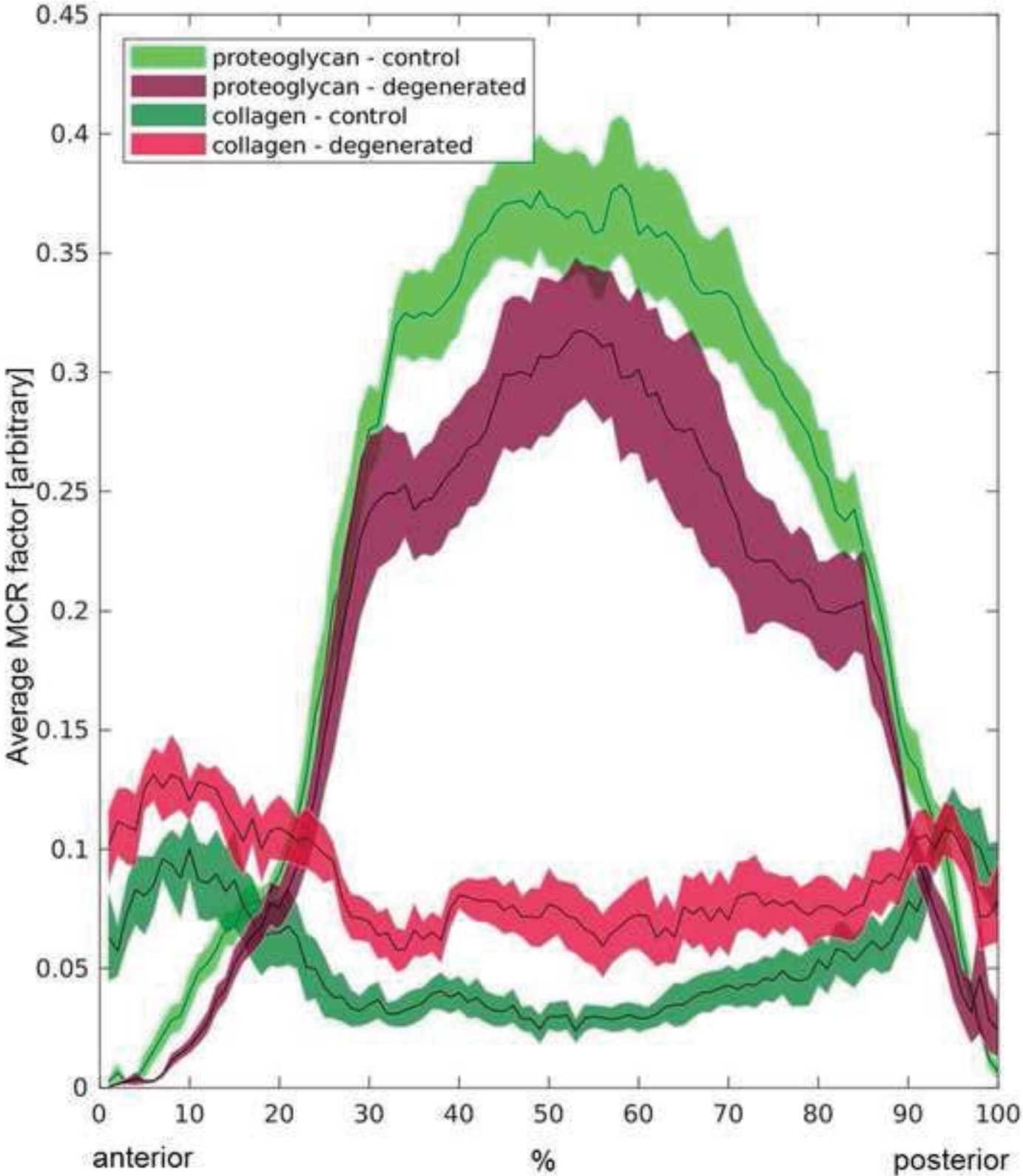


Figure 5  
[Click here to download high resolution image](#)

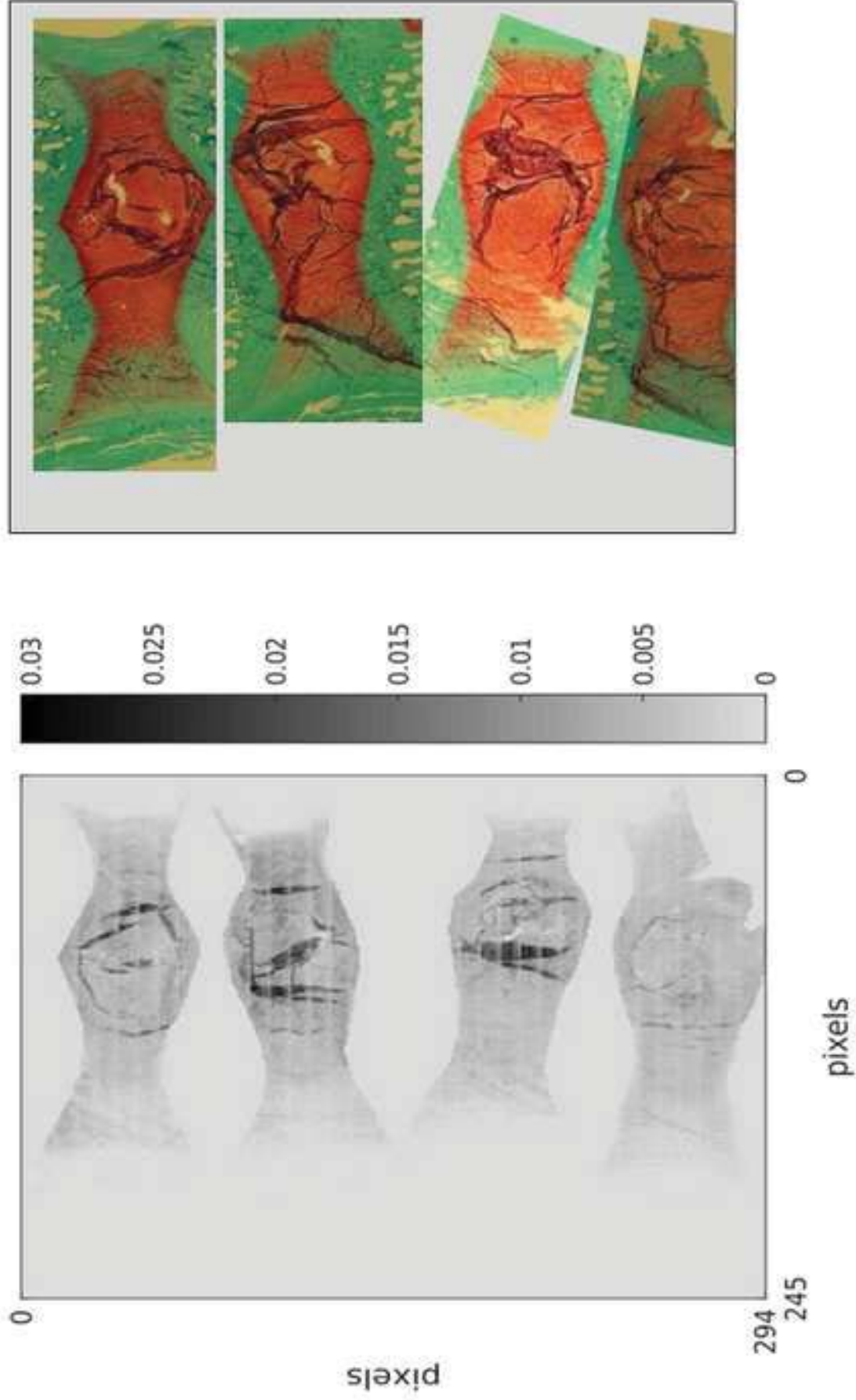


Figure 6  
[Click here to download high resolution image](#)

